

POSSIBLE NEW γ -RAY PULSAR DETECTIONS FOR AGILE AND GLAST MISSIONS: THE OUTER GAP MODEL LOOK AT THE PARKES PULSAR CATALOG

DIEGO F. TORRES[†] & SEBASTIÁN E. NUZA[‡]

[†] Lawrence Livermore National Laboratory, 7000 East Ave. L-413, Livermore, CA 94550, USA

[‡] Departamento de Física J.J. Giambiagi, FCEN, UBA, Pabellón 1, Ciudad Universitaria, 1428 Buenos Aires, Argentina

ABSTRACT

The predictive power of the outer gap model of high energy emission from pulsars is used to analyze the Parkes Multibeam pulsar survey. We find that most of the radio pulsars of the Parkes catalog are not γ -ray emitters according to the outer gap model. The sample of possible new γ -ray pulsar detections for AGILE and GLAST is given. That includes thirteen new excellent candidates. Four new positional coincidences between EGRET detections and Parkes pulsars are found, but for which we discard a physical association. The consequences of applying a new electron density model in assigning the pulsar distances are explored. The new model systematically reduce the distances to the pulsars, corrections can be as large as 90%, increasing their fluxes and affecting the detection prospects.

Subject headings: pulsars: general, gamma-rays: theory, gamma-rays: observations

1. INTRODUCTION

The Parkes multibeam pulsar survey (PMPS, now containing 468 objects) is a large-scale survey of a narrow strip of the inner Galactic plane ($|b| < 5^\circ$, $260^\circ < l < 50^\circ$; Manchester et al. 2001). PMPS pulsars are generally thought to be potential counterparts of EGRET unidentified sources. However, only a handful of them are superposed with EGRET detections, and even less can be considered a plausible counterpart (e.g. D’Amico et al. 2001; Camilo et al. 2001; Torres et al. 2001b). PMPS pulsars are also thought of as natural candidates for new γ -ray detections by AGILE and GLAST missions. Nevertheless, this is strongly dependent on the high energy emission model assumed. Predicting which pulsars can (or cannot) be emitting γ -rays is essential in determining if these models are correct.

2. THE OUTER GAP MODEL LOOK AT THE PARKES CATALOG

There are basically two kinds of models for high energy emission from pulsars. In polar cap models, charged particles are accelerated in charged-depleted zones near the poles of the pulsar. γ -rays are produced through curvature-radiation-induced γ -B pair cascades (Harding 1981) or Compton-induced pair cascades (Dermer & Sturmer 1994). For outer gaps, particle acceleration occurs in charged-depleted regions in the outer magnetosphere. There are two outer gap models: thin and thick outer gaps. Here we shall use the thick outer gap scenario because it can be applied to all radio pulsars, including mature ones (this is the case of most pulsars in our sample, whose mean characteristic age is 500 kyr).

In the thick outer gap model (Zhang & Cheng 1997), the size of the outer gap, f_s , is limited by pair production between the soft thermal X-rays from the stellar surface and the curvature photons with energy $E_\gamma(f_s)$ emitted by the primary e $^\pm$ accelerated in the gap. The energy of the soft X-ray photons, $E_X(f_s)$, is determined by the backflow of the gap’s e $^\pm$. Therefore $E_X(f_s)$ is also a function of the gap size. Using $E_X(f_s)E_\gamma(f_s) \sim (mc^2)^2$, the size of the outer gap (the ratio between the outer gap volume and R_L^3 , with R_L the light cylinder radius) is: $f_s = 5.5P^{26/21}B_{12}^{-4/7}$, where P is the pulsar period and B_{12} the magnetic field in units

of 10^{12} G (see Zhang & Cheng 1997; Zhang & Cheng 1997; 1998a,b for details). It should be noted that f_s is bound to be less than 1 for this model to make sense. The γ -ray luminosity is: $L_\gamma \sim 3.6 \times 10^{31} f_s^3 B_{12}^2 P^{-4}$ erg s $^{-1}$. The integrated flux on Earth is then given by

$$F_\gamma^{th} \sim \frac{L_\gamma}{\Delta\Omega d^2 \bar{E}_c} \sim \frac{7 \times 10^{-7}}{d_{kpc}^2 \Delta\Omega} \left(\frac{B_{12}}{P} \right)^{11/28} \text{ ph cm}^{-2} \text{ s}^{-1}. \quad (1)$$

Here, \bar{E}_c is an average energy of the radiated photons, $\bar{E}_c \sim 10^{-3}(P/B_{12})^{3/28}$ erg, $\Delta\Omega$ is the beaming angle, and d the distance to the pulsar. The theoretical efficiency of the model $\eta_{th} = L_\gamma/\dot{E}$ results in $\eta_{th} \sim 83B_{12}^{-12/7}P^{26/7}$. These formulae has been compared with data for the observed γ -ray pulsars, and for 350 radio pulsars with ages above 1 kyr and known γ -ray flux upper limits (Zhang & Cheng 1998a, see also Zhang et al. 2000). Zhang & Cheng (2002) have considered the outer gap model in relation with the soft gamma-ray repeaters, and Anchordoqui et al. (2002) used an outer gap scenario to study the neutrino production in X-ray binaries.

Tables 1 and 2 show PMPS pulsars for which $f_s < 1$. Columns show the pulsar name, the period and period derivative, the characteristic age $\tau = P/2\dot{P}$, the spin-down luminosity ($\dot{E} = 4\pi^2 I \dot{P}/P^3$, with $I = 10^{45}$ g cm 2), the magnetic field (assuming a dipole model, $\dot{E} = 2.8 \times 10^{31} B_{12}^2 P^{-4}$ erg s $^{-1}$, with B_{12} being the magnetic field in units of 10^{12} G), the distance (obtained using the model by Taylor and Cordes 1993), f_s , the theoretical expected efficiency, the γ -ray luminosity, the flux on Earth (assuming 1 sr beaming), and the comparison of the predicted flux with the sensitivity of forthcoming satellites. A y-mark represents that the flux is above AGILE (GLAST) sensitivity, considered as 5×10^{-8} (2×10^{-9}) photons cm $^{-2}$ s $^{-1}$, respectively. It is clear that different beaming fractions can change the verdict on which pulsar will be possible to observe. Thus, the detection marks y and n are only indicative of what can one expect, but are not to be considered final predictions. On the contrary, PMPS pulsars not contained in these tables are unable to produce γ -rays if the outer gap model is correct, no matter any other possible uncertainty in distance or beaming angle.

Table 1 contains pulsars for which the efficiency is less than 20%, as for the observed 3EG γ -ray pulsars. Table 2 lists pulsars which have $f_s < 1$, but produce much larger values of theoretical efficiencies. 60% of these pulsars have $\dot{E}_{33}/d^2 < 0.5$, which has been often used as an indicator for a low probability of detection (e.g. Thompson et al. 2001). While these pulsars could still be plausible outer gap γ -ray pulsar candidates from a strictly theoretical point of view, they are not phenomenologically favored.

In the thick outer gap model given by Zhang & Cheng (1997), the effects of magnetic inclination angle (α) are not taken into account (Zhang & Cheng 2002). Under these effects, f_s transforms into $f_s \times c(\alpha)$ where $c(\alpha) = 1, 0.9, 0.83, 0.70, 0.57$ for inclination angles of 45, 55, 65, and 75 degrees (Cheng 2002). However, although f_s will vary with α , its value at $R_L/2$, where R_L is the radius of light cylinder (see Cheng, Ruderman & Zhang, 2000) is a sensible approximation. In addition, most of the Parkes pulsars having $f_s > 1$ have indeed $f_s \gg 1$, and so the α -dependence is unimportant here.

3. PULSAR DISTANCES

The distances given in the PMPS were obtained applying the model for the Galactic distribution of electrons given by Taylor and Cordes (1993). Recently, Cordes and Lazio (2002) presented an improved model for this distribution. We have used Cordes and Lazio's (2002) NE2001 code to compute these new distances using the dispersion measures given in the PMPS. Fig. 1a shows how they deviate from the previous estimations for all pulsars contained in Tables 1 and 2. Generally, new inferred values are smaller, what implies bigger fluxes, see Fig. 1b. For some particular cases -especially for those pulsars having the largest inferred 1993 distances- differences are notorious. Tables 1 and 2 give, as well, the newly computed distances and fluxes (separated by a /-symbol). These values affect the detection criterion for the AGILE mission. Using the newest electron model, there are 14% more $f_s < 1$ pulsars with fluxes above the AGILE threshold. Note, however, that changing the distances to these new values does not affect the sample of possible outer gap pulsars: The latter is constructed using only intrinsic pulsar parameters.

4. POSITIONAL COINCIDENCES

There are four EGRET sources now found to be spatially coincident with newly discovered PMPS pulsars. Table 3 shows these new positional coincidences, obtained using FORREST (Sigl et al. 2001). In all these cases, the efficiencies required to produce the γ -ray sources are $\eta \gg 1000\%$ (even for the reduced

NE2001 distances), making the potential associations unphysical. None of the pulsars contained in Table 3 has $f_s < 1$.

The possibly variable source (Torres et al. 2001) 3EG J1824–1514 has been proposed to be result of inverse Compton emission from a microquasar (Paredes et al. 2000). Although there are (considering all catalogs) three pulsars coincident with this source none pose a challenge for the microquasar interpretation. There are three pulsars in the 3EG J1903+0550 error box, but none is energetic enough as to produce it. 3EG J1903+0550 is also coincident with SNR G39.2–0.3 (Romero et al. 1999), which is in turn co-spatial with a giant molecular cloud. Torres et al. (2002) have shown that the interaction between the molecular cloud and the SNR could produce most of the flux observed by EGRET, similar to the case of G347.3-0.5 (Butt et al. 2001).

5. CONCLUDING REMARKS

In the framework of the outer gap model of γ -ray emission from pulsars, we have theoretically computed the γ -ray luminosity, the theoretical efficiency, and other parameters for all radio pulsars listed in the current version of the PMPS. Most pulsars (82% out of 468 reported in the latest release) are not γ -ray pulsars if the outer gap model is correct. Should AGILE or GLAST detect γ -ray emission coming from PMPS pulsars not contained in Tables 1 and 2, a different high energy emission should be operative. This is a definite prediction valid independently of our ignorance of the beaming angle or the distance. Tables 1 and 2 then show PMPS pulsars which, in the framework of the outer gap model, can be γ -ray detections for AGILE and GLAST. 13 of these pulsars are excellent candidates, having large values of \dot{E} and \dot{E}_{33}/d^2 , and low values of f_s and η_{th} . The new model for the electron density in the galaxy (Cordes and Lazio 2002) reduce the pulsar distances reported in the PMPS, enlarging the predicted fluxes. The use of this new model is essential in determining the expected detection; corrections can be as large as 90%. Finally, four new PMPS pulsars are coinciding with previously detected EGRET sources. None of them qualify as a possible counterpart for their respective spatially coincident γ -ray source, nor they can emit γ -rays if the outer gap model is correct.

The work of D.F.T. was performed under the auspices of the U.S. D.O.E. (NSA), by University of California Lawrence Livermore National Laboratory under contract No. W-7405-Eng-48. D.F.T. is LLNL's Lawrence Fellow in Astrophysics. He thanks F. Camilo, G.E. Romero, C. Mauche, and K.S. Cheng for useful comments.

REFERENCES

- Anchordoqui L., et al. 2002, hep-ph/0211231.
- Butt Y.M., et al. 2001, ApJ 562, L167
- Camilo F., et al. 2001, ApJ 557, L51
- Cheng K.S. 2002, Talk at the COSPAR Symposium on high energy emission from SNRs, Houston, October 10-13
- Cheng K.S., Ruderman M. & Zhang L. 2000, ApJ 537, 964
- Cordes J.M., & Lazio T.J.W., astro-ph/0207156
- D'Amico N., et al. 2001, ApJ 552, L45
- Dermer C.D. & Sturmer S.J. 1994, ApJ 420, L79
- Harding A.K. 1981, ApJ 245, 267
- Manchester R.N., et al. 2001, MNRAS 328, 17. Updates at <http://www.atnf.csiro.au/research/pulsar/pmsurv>
- Paredes J.M., Martí J., Ribó M., Massi M., 2000, Science 288, 2341
- Ribó M., et al. 2002, A&A 384, 954
- Romero G.E., Benaglia P., Torres D.F. 1999 A&A 348, 868
- Sigl G., Torres D.F., Anchordoqui L.A., & Romero G.E. 2001, Phys. Rev. D63, 081302
- Taylor J.H., & Cordes J.M. 1993, ApJ, 411, 674
- Thompson D.J. 2001, High Energy Gamma-Ray Astronomy, International Symposium held 26-30 June, 2000, in Heidelberg, Germany. American Institute of Physics (AIP) Proceedings, volume 558. Edited by F. A. Aharonian and H. J. Völk. Published by AIP, Melville, New York, p.103
- Torres D.F., et al. 2001, A&A 370, 468
- Torres D.F., et al. 2002, astro-ph/0209565
- Torres D.F., Butt Y.M., & Camilo F.C. 2001b, ApJ 560, L155
- Zhang L. & Cheng K.S. 1997, ApJ 487, 370
- Zhang L. & Cheng K.S. 1998a, MNRAS 294, 177
- Zhang L., & Cheng, K.S. 1998b, A&A, 335, 234
- Zhang L., & Cheng, K.S. 2002, ApJ, 579, 716
- Zhang L., Zhang, Y.J., & Cheng, K.S. 2000, A&A 357, 957

TABLE 1

PARKES PULSARS WITH $f_s < 1$ AND $\eta_{th} < 0.2$. THOSE PULSARS HAVING A STAR PRESENT $\dot{E} > 10^{36}$ ERG s $^{-1}$, $\dot{E}_{33}/d^2 \gg 0.5$, AND VERY LOW VALUES OF f_s AND η_{th} . THOSE WITH A † -SYMBOL ARE IN COINCIDENCE WITH EGRET SOURCES.

Pulsar J	P ms	\dot{P} 10^{-15}	τ kyr	\dot{E} 10^{33} erg s $^{-1}$	B 10^{12} G	d kpc	f_s	η_{th}	L_γ 10^{33} erg s $^{-1}$	$F_{th}^{\Delta\Omega=1}$ 10^{-8} cm $^{-2}$ s $^{-1}$	A?	G?
J0834–4159	121	4.4	432.8	98.6	0.9	9.7/1.6	0.43	0.04	10.5	1.6/58.9	n/y	y
J0855–4644*	65	7.3	141.2	1059.3	0.8	9.9/3.8	0.21	< 0.01	12.3	1.9/12.9	n/y	y
J0901–4624	442	87.5	80.1	40.0	7.3	7.4/2.8	0.64	0.13	13.3	3.8/26.9	n/y	y
J0940–5428*	88	32.9	42.2	1933.9	2.0	4.2/2.9	0.18	< 0.01	14.6	13.1/28.4	y/y	y
J1015–5719 †	140	57.4	38.7	827.5	3.3	4.8/5.0	0.24	0.00	14.8	10.2/9.6	y/y	y
J1016–5819	88	0.7	1995.1	40.7	0.3	4.6/4.7	0.54	0.08	8.4	5.3/5.1	y/y	y
J1016–5857 †*	107	80.6	21.1	2570.5	3.4	9.3/8.0	0.17	< 0.01	16.1	3.1/4.1	n/n	y
J1019–5749	162	20.1	128.3	184.7	2.1	30.0/6.9	0.37	0.02	12.5	0.2/3.7	n/n	y
J1052–5954	181	20.0	143.3	133.9	2.2	13.5/8.5	0.41	0.03	12.3	1.0/2.5	n/n	y
J1112–6103*	65	31.5	32.7	4530.4	1.7	30.0/12.2	0.13	< 0.01	15.2	0.3/1.8	n/n	y
J1119–6127*	408	4021.8	1.6	2342.1	47.5	30.0/17.1	0.19	< 0.01	23.3	0.5/1.5	n/n	y
J1138–6207	118	12.5	149.4	303.2	1.4	24.5/9.6	0.31	0.01	12.2	0.3/1.9	n/n	y
J1156–5707	288	26.5	172.9	43.5	3.2	20.4/6.0	0.60	0.10	12.0	0.4/4.6	n/n	y
J1248–6344	198	16.9	185.9	85.6	2.1	23.4/8.3	0.47	0.05	11.8	0.3/2.3	n/n	y
J1301–6305*	185	266.7	11	1676.0	8.2	15.8/7.8	0.20	< 0.01	17.7	1.3/5.3	n/y	y
J1327–6400	281	31.2	142.7	55.7	3.5	30.0/15.4	0.56	0.08	12.3	0.2/0.7	n/n	y
J1406–6121	213	54.7	61.8	223.2	4.0	9.1/8.1	0.36	0.02	13.8	2.7/3.4	n/n	y
J1412–6145 †	315	98.7	50.7	124.3	6.5	9.3/7.8	0.45	0.04	14.2	2.6/3.7	n/n	y
J1413–6141 †	286	333.4	13.6	564.9	11.4	11.0/10.1	0.28	0.01	17.2	2.5/2.9	n/n	y
J1420–6048 †*	68	83.2	13	10359.6	2.8	7.6/5.6	0.11	< 0.01	17.3	5.1/9.6	y/y	y
J1452–5851	387	50.7	120.9	34.6	5.2	5.6/4.3	0.66	0.14	12.6	6.1/10.4	y/y	y
J1509–5850	89	9.2	153.7	514.9	1.1	3.7/2.5	0.26	< 0.01	12.2	13.0/29.7	y/y	y
J1514–5925	149	2.9	818.3	34.5	0.8	4.3/3.5	0.60	0.11	9.6	6.9/10.8	y/y	y
J1524–5625*	78	39.0	31.8	3213.2	2.0	3.8/2.8	0.15	< 0.01	15.2	17.2/32.1	y/y	y
J1531–5610	84	13.7	97.2	908.7	1.3	3.0/2.0	0.22	< 0.01	13.0	21.2/50.1	y/y	y
J1538–5551	105	3.2	517.3	110.4	0.7	10.3/7.4	0.41	0.03	10.2	1.4/2.7	n/n	y
J1541–5535	296	75.0	62.5	114.4	5.5	7.5/5.7	0.45	0.04	13.8	3.9/6.8	n/y	y
J1543–5459	377	52.0	114.9	38.3	5.2	6.3/4.8	0.64	0.13	12.7	4.9/8.4	n/y	y
J1548–5607	171	10.7	252.4	84.9	1.6	6.9/4.8	0.47	0.05	11.3	3.5/7.3	n/y	y
J1601–5335	288	62.4	73.3	102.6	5.0	4.0/4.5	0.47	0.05	13.5	13.1/10.5	y/y	y
J1626–4807	294	17.5	266.7	27.2	2.7	10.2/8.9	0.69	0.16	11.2	1.6/2.1	n/n	y
J1632–4757	229	15.1	240.4	49.8	2.2	7.0/6.3	0.56	0.09	11.4	3.4/4.2	n/n	y
J1632–4818	813	650.4	19.8	47.7	27.0	8.5/7.7	0.64	0.13	16.3	3.8/4.6	n/n	y
J1637–4642 †	154	59.2	41.2	639.6	3.5	5.7/5.1	0.26	< 0.01	14.7	7.2/9.2	y/y	y
J1638–4608	278	51.5	85.6	94.5	4.4	5.8/5.1	0.48	0.05	13.2	6.1/8.0	y/y	y
J1648–4611	165	23.7	110.1	208.9	2.3	5.7/5.0	0.36	0.02	12.7	6.1/7.9	y/y	y
J1702–4128	182	52.3	55.2	342.0	3.6	5.1/4.7	0.32	0.01	14.1	8.5/10.2	y/y	y
J1702–4310	241	223.8	17	634.9	8.6	5.4/5.1	0.27	0.01	16.6	9.6/10.9	y/y	y
J1705–3950	319	60.6	83.4	73.7	5.2	3.8/3.2	0.52	0.07	13.3	14.0/20.3	y/y	y
J1715–3903 †	278	37.7	117.2	68.9	3.8	4.7/4.1	0.52	0.07	12.6	8.7/11.6	y/y	y
J1718–3825*	75	13.2	89.5	1253.7	1.2	4.2/3.6	0.20	< 0.01	13.1	11.5/15.9	y/y	y
J1723–3659	203	8.0	401.4	37.9	1.5	4.2/3.5	0.60	0.11	10.6	8.4/12.5	y/y	y
J1726–3530	1110	1216.8	14.5	35.1	43.1	9.9/8.4	0.72	0.19	17.0	3.0/4.2	n/n	y
J1734–3333	1169	2279.0	8.1	56.3	60.5	7.4/6.4	0.64	0.13	18.5	6.0/8.0	y/y	y
J1735–3258	351	26.1	213.4	23.8	3.5	11.1/9.5	0.72	0.19	11.6	1.4/1.9	n/n	y
J1737–3137	450	138.8	51.5	59.9	9.3	5.8/5.4	0.57	0.09	14.2	6.7/7.9	y/y	y
J1738–2955	443	81.9	85.9	37.1	7.1	3.9/3.4	0.65	0.14	13.2	13.6/17.9	y/y	y
J1739–3023	114	11.4	159	300.9	1.3	3.4/2.9	0.31	0.01	12.1	15.8/21.8	y/y	y
J1743–3153	193	10.6	289.7	57.9	1.7	8.0/6.5	0.53	0.07	11.1	2.5/3.8	n/n	y
J1806–2124	482	118.9	64.2	42.0	8.9	10.0/9.8	0.63	0.13	13.8	2.2/2.2	n/n	y
J1809–1917*	83	25.5	51.4	1779.8	1.7	3.7/3.5	0.18	< 0.01	14.2	16.7/18.7	y/y	y
J1828–1101*	72	14.8	77.1	1563.0	1.2	7.2/6.6	0.18	< 0.01	13.4	4.0/4.8	n/n	y
J1837–0604 †*	96	45.2	33.8	1998.6	2.4	6.1/6.4	0.18	< 0.01	15.1	6.5/6.0	y/y	y
J1838–0453 †	381	115.7	52.2	82.7	7.8	8.2/8.1	0.51	0.06	14.2	3.3/3.4	n/n	y
J1839–0321	239	12.5	302.4	36.3	2.0	6.8/7.2	0.62	0.12	11.0	3.5/3.1	n/n	y
J1843–0355	132	1.0	2017.1	17.7	0.4	8.8/8.8	0.72	0.18	8.4	1.4/1.4	n/n	y
J1853+0056	276	21.4	204.3	40.3	2.8	3.8/5.1	0.61	0.11	11.7	12.0/6.7	y/y	y
J1904+0800	263	17.3	241.1	37.4	2.5	9.2/8.6	0.62	0.12	11.4	2.0/2.3	n/n	y
J1907+0345	240	8.2	463.1	23.4	1.6	8.7/7.1	0.70	0.17	10.4	2.0/3.0	n/n	y
J1908+0909	337	34.9	153	36.1	4.0	8.8/8.9	0.64	0.13	12.2	2.4/2.3	n/n	y
J1909+0912	223	35.8	98.7	127.6	3.3	8.2/8.2	0.43	0.04	12.9	3.0/3.0	n/n	y
J1913+0832	134	4.6	466.2	74.3	0.9	7.7/7.8	0.48	0.05	10.4	2.5/2.4	n/n	y
J1913+1011*	36	3.4	169.1	2871.4	0.4	4.4/4.7	0.14	< 0.01	12.0	9.1/8.2	y/y	y

TABLE 2
ADDITIONAL PARKES PULSARS WITH $f_s < 1$ BUT $\eta_{th} > 0.2$.

Pulsar J	P ms	\dot{P} 10^{-15}	τ kyr	E 10^{33} erg s $^{-1}$	B 10^{12} G	d kpc	f_s	η_{th}	L_γ 10^{33} erg s $^{-1}$	$F_{th}^{\Delta\Omega=1}$ 10^{-8} cm $^{-2}$ s $^{-1}$	A?	G?
J0954–5430	473	43.9	170.7	16.4	5.3	6.2 /3.9	0.83	0.29	12.0	4.7 /11.8	n/y	y
J0957–5432	204	1.9	1657.6	9.1	0.7	7.0 /4.3	0.91	0.37	8.7	2.4 /6.3	n/y	y
J1043–6116	289	10.4	439.8	17.1	2.0	18.1 /9.4	0.78	0.24	10.5	0.4 /1.4	n/n	y
J1115–6052	260	7.2	569.3	16.3	1.6	6.7 /4.1	0.79	0.24	10.1	3.1 /8.4	n/y	y
J1216–6223	374	16.8	352.6	12.7	2.9	30.0 /16.5	0.87	0.33	10.8	0.2 /0.6	n/n	y
J1305–6203	428	32.1	211	16.2	4.3	24.1 /8.5	0.83	0.28	11.6	0.3 /2.4	n/n	y
J1349–6130	259	5.1	802.4	11.6	1.4	5.8 /4.9	0.87	0.32	9.6	4.0 /5.6	n/y	y
J1452–6036	155	1.4	1694.9	15.4	0.6	9.4 /5.8	0.76	0.22	8.6	1.3 /3.4	n/n	y
J1515–5720	287	6.1	745.3	10.2	1.5	10.2 /6.6	0.91	0.37	9.7	1.3 /3.1	n/n	y
J1530–5327	279	4.7	944.4	8.5	1.3	1.4 /1.2	0.95	0.43	9.4	60.8 /90.0	y/y	y
J1618–4723	204	2.0	1619.6	9.3	0.7	3.4 /3.0	0.90	0.37	8.7	9.9 /13.0	y/y	y
J1649–4653	557	49.7	177.6	11.4	6.2	5.1 /4.6	0.94	0.41	11.9	6.8 /8.5	y/y	y
J1649–4729	298	6.5	720.6	9.8	1.6	12.7 /8.0	0.92	0.39	9.7	0.8 /2.0	n/n	y
J1711–4322	103	0.2	7747.6	7.7	0.2	4.1 /3.8	0.89	0.36	6.9	4.9 /5.9	n/y	y
J1812–1910	431	37.7	181.1	18.6	4.7	11.5 /11.2	0.79	0.25	11.9	1.3 /1.3	n/n	y
J1835–1020	302	5.9	810.2	8.4	1.6	2.5 /2.3	0.96	0.45	9.6	20.2 /25.2	y/y	y
J1837–0559	201	3.3	964.6	16.1	1.0	5.0 /5.4	0.77	0.23	9.3	5.1 /4.3	y/n	y
J1842–0905	345	10.5	520.7	10.1	2.2	7.4 /5.9	0.93	0.40	10.2	2.7 /4.2	n/n	y
J1845–0743	105	0.4	4527.9	12.6	0.2	5.9 /5.2	0.77	0.23	7.5	2.7 /3.4	n/n	y
J1853+0545	126	0.6	3279.4	11.9	0.3	4.7 /5.1	0.80	0.26	7.9	4.5 /3.8	n/n	y
J1908+0839	185	2.4	1231.7	14.8	0.8	9.4 /9.2	0.78	0.24	9.0	1.4 /1.4	n/n	y

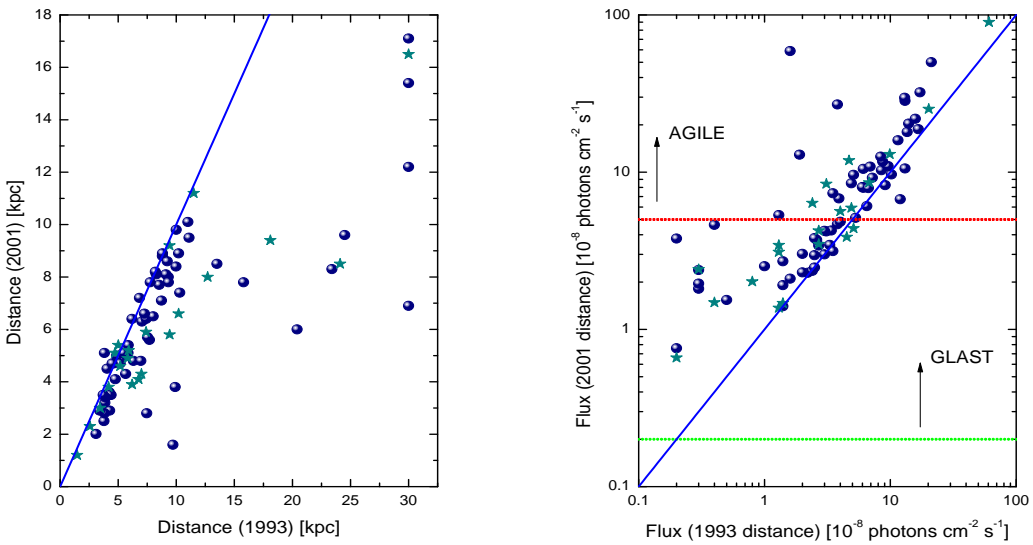


FIG. 1.— Pulsar distances computed using NE2001 and implied variation in fluxes as compared with the 1993 model results. The solid line is, in both plots, the curve $y = x$. Circles represent pulsars in Table 1 ($f_s < 1, \eta_{th} < 0.2$); stars represent pulsars in Table 2 ($f_s < 1, \eta_{th} > 0.2$).

TABLE 3
NEW PARKES PULSARS SPATIALLY COINCIDENT WITH EGRET SOURCES.

EGRET	Pulsar J	P s	\dot{P} 10^{-15}	\dot{E} ergs s $^{-1}$	\dot{E}/d^2 [1993] ergs s $^{-1}$ kpc $^{-1}$	\dot{E}/d^2 [2001] ergs s $^{-1}$ kpc $^{-1}$
1824–1514	1825–1526	1.62	4.2	3.8×10^{31}	4.4×10^{29}	5.8×10^{29}
	1826–1526	0.38	1.0	7.6×10^{32}	6.4×10^{30}	5.1×10^{31}
1903+0550	1905+0616	0.98	135.21	5.5×10^{33}	1.9×10^{32}	1.7×10^{32}
1638–5155	1638–5226	0.34	2.65	2.6×10^{33}	9.8×10^{31}	2.3×10^{32}
1704–4732	1707–4729	0.26	1.5	3.3×10^{33}	2.9×10^{31}	8.5×10^{31}